The Low Pressure Inductive Discharge

Jón Tómas Guðmundsson

Science Institute,

Dunhaga 3, IS-107 Reykjavík

tumi@hi.is

July 12, 2002

Overview

- Partially ionized plasma
- Discharges
- Inductive Discharges
- Planar Inductive Discharge
- Electromagnetic modeling
- Global model of plasma chemistry

Partially ionized plasma

- A plasma is a collection of free charged particles, electrically neutral on the average
- The plasma is either partially or fully ionized gas that contains electrons, ions, neutral atoms and molecules
- In partially ionized plasma discharges charged particles usually interact weakly with each other and electron collisions are most frequent with neutral atoms and molecules
- Ionization of neutrals sustains the plasma in the steady state
- The electrons are not in thermal equilibrium with the ions

Partially ionized plasma

- A plasma is characterized by the plasma parameters, particle equilibrium temperatures and particle densities
- Each species can have its own thermal equilibrium temperature
- Here we will limit the discussion to low pressure discharges
- Low pressure discharges are characterized by
  - $T_{\rm e} \approx 1 - 10$ eV
  - $T_{\rm i} \ll T_{\rm e}$
  - $n_{\rm e} \approx 10^{14} - 10^{19}$ m^{-3}
- The neutral gas pressure is low
  - $p \approx 1$ mTorr – 1 Torr.

Partially ionized plasma

- Low pressure, weakly ionized, non-equilibrium gas discharge plasmas are used for a variety of materials processing applications
- The primary use of plasma processing in the electronics industry is in semiconductor chip manufacturing
- In integrated circuit processing plasma processes are essential in achieving the small feature sizes and packing density required by the electronics industry

Partially ionized plasma

- New high density plasma sources are being developed to meet the requirements for the future integrated circuit devices
- The simplest and most convenient design for a high density discharge for materials processing is the planar inductive discharge which evolved from a century old idea

Discharges

Capacitive discharge

- In the early days capacitively driven radio frequency (rf) discharges were commonly used for dry etching

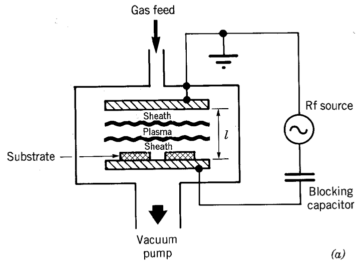

- A conventional capacitively coupled, rf, parallel plate electrode discharge
- Batches of wafers are loaded onto one of the electrodes, either powered or grounded

Discharges

Capacitive discharge

- The typical rf driving voltage is $V_{rf} \approx 100 - 1000$ V operated at 13.56 MHz driving frequency and the electrode separation is $l \approx 2 - 10$ cm
- Typical gas pressures are in the range 10 – 100 mTorr, and plasma densities are relatively low, typically 10^{15} - 10^{17} m^{-3}
- Ion acceleration energy

$$\sim V_{rf}/2$$

- The plasma density is controlled by the applied rf voltage which also determined the ion energy
- No independent control of plasma parameters, such as electron and ion energy, charge density, and reactant density
- The capacitive discharge dominated in the industry until 1994

Discharges

- In the early 1990's plasma processing changed from batch operations to single-wafer operations with 150 mm diameter wafers; wafer sizes are now 300 mm diameter
- For single wafer processing and submicron dry etching, a high plasma density and low neutral gas pressure are desired to obtain the desired profiles and processing rates to compensate for the inherent throughput problem of a single-wafer processing
- This has led to the development of a new generation of low pressure, high-density plasma sources, where the rf or microwave power is coupled to the plasma via a dielectric window

Discharges - Challenges

- High density
  - Higher etch and deposition rates
- Low pressure
  - Reduce scattering (anisotropy)
- Uniformity
  - Larger wafers
- Low and controllable ion energy
  - Radiation damage

Discharges

Electron cyclotron resonance (ECR) discharge

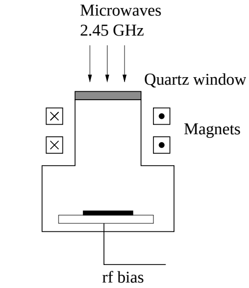

Planar inductively coupled discharge

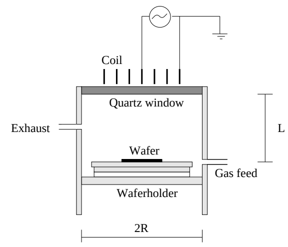

Discharges

- The inductive and ECR discharges give 1 – 2 orders of magnitude ion density than a capacitively coupled discharge
- Ion bombarding energy is about an order of magnitude lower (and is controllable)
- In these new discharges there is independent control of ion density and ion bombarding energy
  - The ion density is controlled by the power applied to the inductive coil (or microwave power)
  - The ion energy can be controlled by rf bias applied to the substrate holder
- Currently the inductive discharge dominates in the electronics industry

Discharges

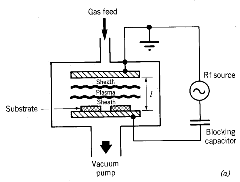

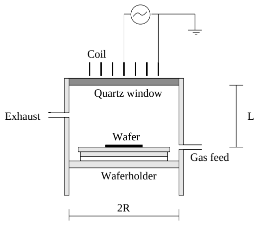

	Capacitive discharge	High density
Gas pressure [mTorr]	10 – 1000	0.5 –50
Power [W]	50 – 2000	100 – 5000
Driving frequency [Mhz]	0.05 – 13.56	0 – 2450
Electron density [cm^{-3}]	10^9 – 10^{10}	10^{10} – 10^{12}
Electron temperature [eV]	1 – 5	2 –7
Ion energy [V]	200 – 1000	< 100

The inductive discharge

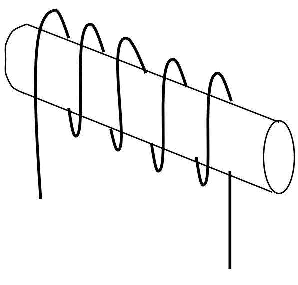

- An inductive discharge in its simplest form is a tube made of quartz or ceramic placed inside a solenoid (the primary coil) through which rf current is applied
- The inductive discharge was introduced by W. Hittorf in 1884 [Hittorf, 1884]
- He describes a method to send a current, induced by another current, through a gas, without electrodes

The inductive discharge

- These early experiments caught the interest of J. J. Thomson who repeated the experiments [Thomson, 1891].
- Consequently Thomson developed a theory assuming a purely inductive coupling mechanism
- The discharge was taken to be a single turn lossy conductor that is coupled to the non-resonant coil
- The discharge forms a secondary loop that has resistance R_2, a self inductance L_2 and a mutual inductance with the primary circuit M

The inductive discharge

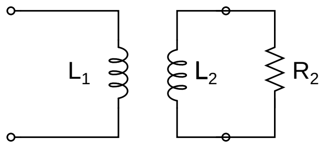

- The resistance change seen in the primary loop due to the discharge loop is then

$$\rho' = \frac{\omega^2 M^2 R_2}{R_2^2 + \omega^2 L_2^2}$$

were ω is the driving frequency of the current in the primary circuit

- N. Tesla was convinced that the discharge was primarily of electrostatic nature, a result of the large potential difference which exists between the ends of the inductive coil [Tesla, 1891]
- The nature of the discharge was a debate for over five decades and is still not fully resolved

The inductive discharge

- MacKinnon [MacKinnon, 1929] resolved this question by demonstrating that as the power is increased, a weak capacitively coupled electrostatic mode (E-mode) precedes the inductively coupled magnetic mode (H-mode).
- The discharge is either maintained by the axial electrostatic field or by an azimuthal electromagnetic field of the inductor coil
- To reach the magnetic mode the applied power and current has to exceed a critical limit
- The electrostatic mode is characterized by a uniform faint glow
- The electromagnetic mode is characterized by a bright ring-like discharge due to the limited skin depth of the exciting field (the periphery glows more brightly)

The inductive discharge

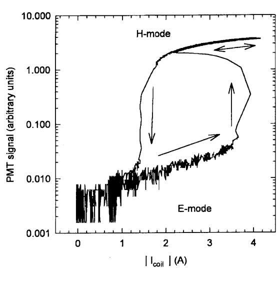

[Kortshagen et al., 1996]

- When the discharge changes from the electrostatic mode to the electromagnetic mode the brightness increases abruptly
- This change in light intensity can be a few orders of magnitude
- Decreasing the applied power dims the discharge emission slightly until an abrupt change to much lower emission occurs

The inductive discharge

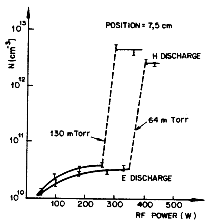

[Amorim et al., 1991]

- The change from electromagnetic mode to electrostatic mode is generally at lower power than the change from electrostatic to electromagnetic mode
- The change in brightness is attributed to the abrupt change in electron density that occurs when the discharge goes through the transition
- This change in density can be from a low density mode $n_e < 10^{17}$ m^{-3} to a high density mode $n_e > 10^{17}$ m^{-3}

The planar inductive discharge

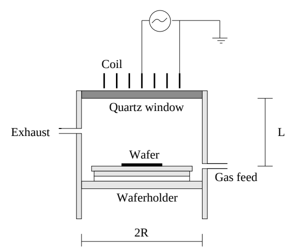

- Around the mid-to-late 1980's inductive systems were introduced to plasma processing
- Their simple design, construction and operation make them attractive for industrial applications such as in etching and deposition processes

The planar inductive discharge

- Other advantages include no need for dc magnetic fields and the use of an rf power source rather than a microwave source
- For materials processing they are often operated in low pressure (< 50 mTorr) and in low aspect ratio geometries, $L/R \leq 1$ for a cylindrical discharge, and can be driven by a planar coil
- The inductive coils are most commonly driven at 13.56 MHz or below, using a 50 Ω rf power supply through a capacitive matching network
- An electrostatic shield is often placed between the coil and the plasma to reduce possible capacitive coupling

The planar inductive discharge

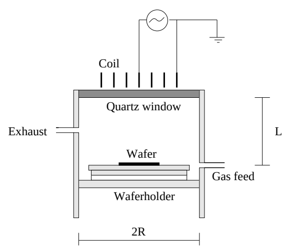

- The substrate may be placed in close proximity to the inductive coil
- In the planar configuration the coil is typically separated from the plasma by a 1 – 3 cm thick quartz window and the substrate is placed 5 – 10 cm below the window (3 - 10 skin depths)

The planar inductive discharge

- The inductive power transfer and lack of electrodes leads to low voltages across all plasma sheaths and wall surfaces
- The dc plasma potential and hence the ion acceleration energy is typically 20 – 40 V at all surfaces
- To control the ion energy the substrate is placed on an electrode that can be independently driven by a capacitively coupled rf source
- Thus there is an independent control of the ion/radical fluxes (through the inductive source power) and the ion-bombarding energy (through the substrate electrode)

Electromagnetic modeling - Power transfer

Primary goal:

- Relate the plasma parameters (electron density and temperature) to the external electrical characteristics of the discharge such as the rf current and rf voltage

Method:

- Apply Thomson's transformer model of the inductive discharge
- Develop a first principles model of the components of the transformer circuit
- Use a global model of the plasma chemistry to estimate the plasma parameters

Electromagnetic modeling - Power transfer

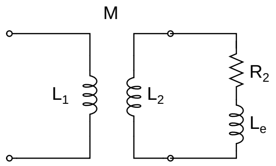

- L_2 is the geometric inductance of the plasma
- L_e is the inertia inductance
- R_2 is the plasma resistance
- M is the mutual inductance between the primary and secondary circuit

Electromagnetic modeling

- Seen in the primary circuit the effect of the coupled secondary circuit is to add the impedance

$$Z_2(\omega M)^2/|Z_2|^2$$

to the primary circuit, where

$$Z_2 = R_2 + j\omega\left[\omega L_2 + \omega L_{\mathrm{e}}\right]$$

is the complex impedance of the secondary circuit

Electromagnetic modeling

- For a planar inductively coupled discharge the magnetic induction components $B_r(r,z)$ and $B_z(r,z)$, the electric field component $E_\theta(r,z)$ and the plasma current are calculated assuming axisymmetric geometry
- The mutual inductance between the primary and secondary circuit M, the self inductance of the plasma L_2 and the impedance of the plasma are determined theoretically and related to the properties of the plasma
- The planar inductive discharge is modeled as a transformer with the inductive coil taken as the primary circuit and the plasma as the secondary circuit to find the impedance characteristics in the primary circuit due to plasma load.

Electromagnetic modeling

- Plasma resistance

$$R_2 \sim f(\nu_{\mathrm{eff}}, n_{\mathrm{e}}, \text{electric field profile})$$

- Effective collision frequency

$$\nu_{\mathrm{eff}} = \nu_{\mathrm{en}} + \nu_{\mathrm{st}} + \nu_{\mathrm{ei}}$$

- Electron density and temperature are related to pressure and applied power via the global (volume averaged) model
- Electron inertia inductance

$$L_{\mathrm{e}} = R_2 \frac{\omega_{\mathrm{eff}}}{\omega} \nu_{\mathrm{eff}}$$

Electromagnetic modeling

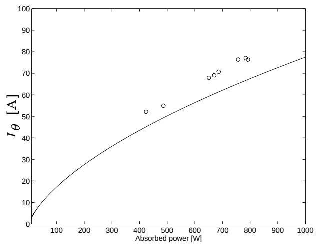

- The induced plasma current I_θ versus the absorbed power for argon plasma at 120 mTorr neutral gas pressure, driving frequency $f = 0.56$ MHz and dimensions $R = 16$ cm and $L = 20$ cm

  $I_\theta = (P_{\text{abs}}/R_2)^{1/2}$

  $E_\theta = E_{\theta \text{o}} J_1(\gamma_1 r) \exp(-z\gamma)$

- The solid line shows the model estimate and the circles the measured data (from [El-Fayoumi, 1996])

Electromagnetic modeling

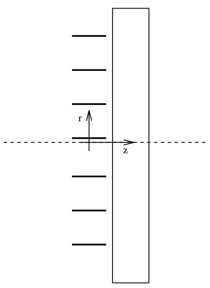

- The vector potential for each of the N turns of the coil, $A_{\theta i}(r, z)$, is given as

$$A_{\theta i}(r, z) = \frac{\mu_\text{o}}{\pi} \frac{I_{rf}}{\kappa_i} \left(\frac{a_i}{r}\right)^{1/2}$$

$$\times \left[\left(1 - \frac{1}{2}\kappa_i^2\right) K(\kappa_i) - E(\kappa_i) \right]$$

- Here a_i, $i = 0, 1, ..., N - 1$ are the mean radii of each of the N turns of the inductive coil and r is the radial position as measured from the axis of the system

Electromagnetic modeling

- The magnetic induction along the axis

$$B_{zi}(r, z) = \frac{\mu_\text{o} I_{rf}}{2\pi} \frac{1}{((a_i + r)^2 + z^2)^{1/2}}$$

$$\times \left[K(\kappa_i) + \frac{a_i^2 - r^2 - z^2}{(a_i - r)^2 + z^2} E(\kappa_i) \right]$$

  and in the radial direction

$$B_{ri}(r, z) = \frac{\mu_\text{o} I_{rf}}{2\pi} \frac{z}{r\,((a_i + r)^2 + z^2)^{1/2}}$$

$$\times \left[-K(\kappa_i) + \frac{a_i^2 + r^2 + z^2}{(a_i - r)^2 + z^2} E(\kappa_i) \right]$$

  where $K(\kappa_i)$ and $E(\kappa_i)$ are the complete elliptic integrals of the first and second kinds respectively

- The parameter κ_i is defined by

$$\kappa_i^2 \equiv \frac{4 a_i r}{z^2 + (a_i + r)^2}$$

Electromagnetic modeling

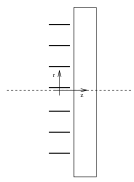

- The axial distance d from the plane of the coil to the plasma is given by

$$d = \frac{\xi_1}{2} + w_g + w_q + \zeta$$

  where

  - ξ_1 is the width of the copper strip that forms the primary coil
  - w_g is the gap size between the near edge of the primary coil and the quartz window
  - w_q is the quartz window thickness
  - ζ is the distance from the quartz/plasma boundary into the plasma

Electromagnetic modeling

- We will normally take $\zeta = \delta/2$, where δ is the skin depth in the plasma
- Assuming cylindrical symmetry, we have

$$E_\theta(r,z) = -\frac{1}{r}\int_{\mathrm{o}}^{r} r'\dot{B}_z(r',z)dr'$$

Electromagnetic modeling

- Because the skin depth δ is small compared to typical axial and radial scale lengths, we can write the plasma current density

$$J_\theta(r,z) \approx K_\theta(r)/\delta$$

  where $K_\theta(r)$ is modeled as the surface current density on a perfectly conducting plane located at $z = d$

$$K_\theta(r) = \frac{2B_r(r)}{\mu_{\mathrm{o}}}$$

- The azimuthal plasma current flowing outside a radius r is then expressed as

$$I_\theta(r) = \int_r^\infty K_\theta(r')dr'$$

  and the total azimuthal plasma current is then $I_{\theta o} = I_\theta(0)$ where

$$I_{\theta 0} = I_{rf}\left(N - \sum_{i=0}^{N-1}\frac{d}{(a_i^2+d^2)^{1/2}}\right)$$

Electromagnetic modeling

- The mutual inductance is found by integrating the flux from the inductive coil linking the plasma current in the discharge over all radii

$$M = \frac{2\pi}{I_{rf}I_{\theta o}}\int_0^\infty rB_z(r,d)I_\theta(r)dr$$

- The self inductance

$$L_2 = \frac{2\pi}{I_{\theta o}^2}\int_0^\infty A_\theta(r',z)K_\theta(r',z)r'dr'$$

- R_2 and L_{e} are determined by the electrical properties of the plasma which are described by the plasma conductivity

$$\sigma_{\mathrm{p}} = \frac{e^2 n_{\mathrm{e}}/m}{\nu_{\mathrm{eff}} + j\omega_{\mathrm{eff}}}$$

  where ν_{eff} is the effective collision frequency, n_{e} is the electron density and ω_{eff} is the effective driving frequency

Electromagnetic modeling

- The current profile is assumed to be related to the electric field by Ohm's law $J_\theta = (\sigma_p + j\omega\epsilon_{\mathrm{o}})E_\theta$ where the electric field is assumed to follow

$$E_\theta(r,z) \propto E_{\theta o}\exp(-z\gamma)$$

- In our regime, the displacement current is much less than the conduction current and

$$P_{\mathrm{abs}} = 2\pi\int_0^\infty dz\int_0^R rdr\mathrm{Re}[\sigma_p]|E_\theta(r,z)|^2$$

- The rms current flowing through the current path is found by integrating the current density over the cross section of this current path or

$$I_\theta = \int_0^\infty dz\int_0^R dr\sigma_p E_\theta(r,z)$$

Electromagnetic modeling

- The resistance of the plasma is then given using $P_{abs} = R_2|I_\theta|^2$ as

$$R_2 = \frac{P_{\rm abs}}{|I_\theta|^2} = \frac{\pi|\gamma|^2}{{\rm Re}[\gamma]}\frac{{\rm Re}[\sigma_{\rm p}]}{|\sigma_{\rm p}|^2}\frac{\int_{\rm o}^R rdr|A_\theta^2(r)|}{\left|\int_{\rm o}^R drA_\theta(r)\right|^2}$$

- The electron inertia inductance is found from

$$L_{\rm e} = \frac{R_2}{\nu_{\rm eff}}\frac{\omega_{\rm eff}}{\omega}$$

Electromagnetic modeling

- Seen in the primary circuit assuming a purely inductive operation, the change in plasma resistance is given by

$$\rho = \frac{\omega^2 M^2 R_2}{R_2^2 + (\omega L_{\rm e} + \omega L_2)^2}$$

- The change in plasma reactance by

$$\chi = -\frac{\omega^2 M^2(\omega L_2 + \omega L_{\rm e})}{R_2^2 + (\omega L_{\rm e} + \omega L_2)^2}$$

- The equivalent impedance of the primary coil and the plasma as seen in the primary circuit is

$$Z_s = R_{\rm o} + \rho + j\omega(L_{\rm o} - \chi)$$

where $R_{\rm o}$ is the resistance and $L_{\rm o}$ is the inductance of the primary coil

Electromagnetic modeling

- There is a high voltage across the inductive coil
- Between the coil and the plasma is a dielectric window which acts as a capacitor
- Next to the window a sheath is expected to form with per unit area capacitance $\sim \epsilon_{\rm o}/s_m$ where s_m is the sheath thickness
- In addition there is both ohmic dissipation within the plasma and stochastic dissipation in the plasma sheath

Electromagnetic modeling

- The capacitive terms appear in parallel with the impedance of the coil and the plasma Z_s

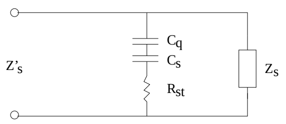

- The effective impedance seen in the primary circuit when the plasma is lit becomes

$$Z_s' = \frac{Z_s Z_{cap}}{Z_s + Z_{cap}}$$

where

$$Z_{cap} = R_{\rm st} + \frac{1}{j\omega C_s} + \frac{1}{j\omega C_q}$$

where

  - $R_{\rm st}$ is the stochastic heating resistance
  - $C_{\rm s}$ is the sheath capacitance
  - $C_{\rm q}$ is the quartz window capacitance

Electromagnetic modeling

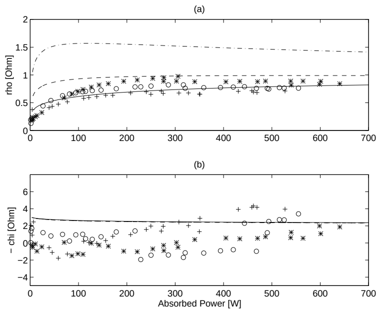

[Gudmundsson and Lieberman, 1998]

- The changes in primary resistance due to capacitive coupling and plasma loading, ρ_{eff}
- The negative of the change in primary reactance due to capacitive coupling and plasma loading $-\chi_{\text{eff}}$,
- Argon plasma at — 2 mTorr, - - 10 mTorr and – · – 60 mTorr, compared to measured values for argon plasma

Electromagnetic modeling

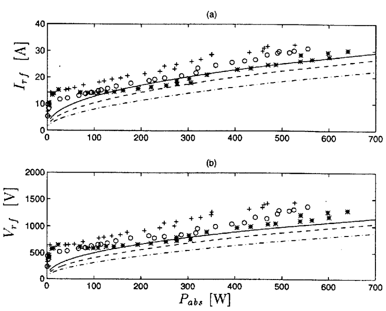

[Gudmundsson and Lieberman, 1998]

- The rms rf current I_{rf} applied to the primary coil versus the power absorbed within the plasma
- The rms rf voltage V_{rf} applied to the primary coil versus the power absorbed within the plasma
- Argon plasma at — 2 mTorr, - - 10 mTorr and – · – 60 mTorr

Plasma chemistry

- The plasma is either partially or fully ionized gas that contains electrons, ions, neutral atoms and molecules
- The electrons are not in thermal equilibrium with ions and molecules in partially ionized plasma

The plasma chemistry can be complicated

Argon discharge consist of

e, Ar, Ar^+, Ar^*,...

Oxygen discharge consist of

e, O, O_2, O_2^+, O^+, O_2^-, O^-, O_2^*, O^*, ...

SF_6 discharge consist of

e, SF_6, SF_5^+, SF_4^+, SF_3^+, F^+, F^-, F^*, F_2, F,....

Global model

The global model is based on:

- Power equilibrium
- Particle conservation for all particles

For argon plasma (noble gas):

Power balance

- Absorbed power = Power loss
- $P_{\text{abs}} = e n_0 u_{\text{B}} A_{\text{eff}} \mathcal{E}_{\text{T}}$

Particle balance

- Particle loss at surface = Ionization in bulk
- $n_0 u_{\text{B}} A_{\text{eff}} = k_{\text{iz}} n_{\text{g}} n_0 \pi R^2 L$

Global model

Energy loss

The total energy loss for each ion that is lost is

$$\mathcal{E}_{\mathrm{T}} = \mathcal{E}_{\mathrm{c}} + \mathcal{E}_{\mathrm{e}} + \mathcal{E}_{\mathrm{i}}$$

where

- $\mathcal{E}_{\mathrm{c}}$ is the collisional energy loss per electron-ion pair created

$$\mathcal{E}_{\mathrm{c}} = \mathcal{E}_{\mathrm{iz}} + \sum_{\mathrm{i}} \mathcal{E}_{\mathrm{ex,i}} \frac{k_{\mathrm{ex,i}}}{k_{\mathrm{iz}}} + \frac{k_{\mathrm{el}}}{k_{\mathrm{iz}}} \frac{3m_{\mathrm{e}}}{m_{\mathrm{i}}} T_{\mathrm{e}}$$

- $\mathcal{E}_{\mathrm{e}}$ is the average energy of each electron that is lost. If we assume the electron energy to be Maxwellian $\mathcal{E}_{\mathrm{e}} = 2T_{\mathrm{e}}$
- $\mathcal{E}_{\mathrm{i}}$ is the average kinetic energy of ions that are lost and is determined by the sheath potential

Global model

Rate coefficients

- Rate coefficients are calculated from cross sections assuming Maxwellian electron energy distribution

$$k = \left(\frac{2e}{m_{\mathrm{e}}}\right)^{1/2} \int_0^\infty \mathcal{E}^{1/2} \sigma(\mathcal{E}) f(\mathcal{E}) d\mathcal{E}$$

Collisional energy loss

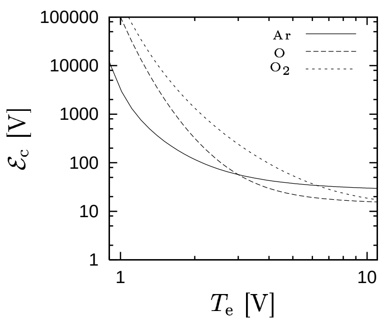

- The collisional energy loss per electron-ion pair created $\mathcal{E}_{\mathrm{c}}$

Global model

Advantages

- Give estimate of the plasma parameter with relatively simple calculations ($n_{\mathrm{e}}, T_{\mathrm{e}}, V_{\mathrm{pl}}, n_{\mathrm{i}}$)
- Tool to estimate which reactions are of importance in particular mixtures

Limiting factors

- Does not give spatial distribution
- The electron energy distribution is given

Oxygen discharge

- Oxygen is relatively simple diatomic molecule
- The oxygen discharge is weakly electronegative, (negative ions O^-, O_2^- and O_3^-)
- Negative ions have a significant influence on the discharge due to recombination in the bulk

For electronegative molecular discharge:

- Particle balance
- Quasi neutrality

$$n_{\mathrm{e}} + \sum_i^{N_-} n_{-,i} = \sum_j^{N_+} n_{+,j}$$

- Power balance

$$\frac{P_{\mathrm{abs}}}{V} = e\sum_i^{N_0} \mathcal{E}_{\mathrm{c}}^{(\mathrm{X})} k_{\mathrm{iz}} n_{\mathrm{X}} n_{\mathrm{e}} + e\sum_i^{N_+} k_{\mathrm{loss}} (\mathcal{E}_{\mathrm{e},i} + \mathcal{E}_{\mathrm{i},i}) n_{\mathrm{X}+,j}$$

J T Gudmundsson *et al*

Table 1. The reaction set for oxygen. The rate coefficients for electron impact collisions were calculated assuming Maxwellian electron energy distribution and fitted over an electron temperature range 1–7 eV.

Reaction	Rate coefficient	Reference
$e + O_2 \longrightarrow O_2^+ + 2e$	$k_1 = 9 \times 10^{-16} T_e^2 \exp(-12.6/T_e)$ m^3 s^{-1}	[23]
$e + O_2^+ \longrightarrow O(^3P) + O(^3P)$	$k_2 = 2.2 \times 10^{-13}$ m^3 s^{-1}	[11]
$e + O_2 \longrightarrow O(^3P) + O^-$	$k_3 = 8.8 \times 10^{-17} \exp(-4.4/T_e)$ m^3 s^{-1}	[46]
$e + O(^3P) \longrightarrow O^+ + 2e$	$k_4 = 9.0 \times 10^{-15} T_e^{0.7} \exp(-13.6/T_e)$ m^3 s^{-1}	[46]
$O^- + O_2^+ \longrightarrow O(^3P) + O_2$	$k_5 = 1.5 \times 10^{-13} (300/T_g)^{1/2}$ m^3 s^{-1}	[23]
$O^- + O^+ \longrightarrow O(^3P) + O(^3P)$	$k_6 = 2.7 \times 10^{-13} (300/T_g)^{1/2}$ m^3 s^{-1}	[11]
$e + O^- \longrightarrow O(^3P) + 2e$	$k_7 = 1.1 \times 10^{-13} \exp(-3.58/T_e)$ m^3 s^{-1}	[47]
$e + O_2 \longrightarrow O(^3P) + O(^3P) + e$	$k_8 = 7.1 \times 10^{-15} \exp(-8.6/T_e)$ m^3 s^{-1}	[11]
$O(^3P) + O^- \longrightarrow O_2 + e$	$k_9 = 3.0 \times 10^{-16} (300/T_g)^{1/2}$ m^3 s^{-1}	[46]
$e + O_2 \longrightarrow O^- + O^+ + e$	$k_{10} = 7.1 \times 10^{-17} T_e^{0.5} \exp(-17/T_e)$ m^3 s^{-1}	[46]
$e + O_2 \longrightarrow O(^3P) + O^+ + 2e$	$k_{11} = 5.3 \times 10^{-16} T_e^{0.9} \exp(-20/T_e)$ m^3 s^{-1}	[46]
$O^+ + O_2 \longrightarrow O(^3P) + O_2^+$	$k_{12} = 2 \times 10^{-17} (300/T_g)^{1/2}$ m^3 s^{-1}	[11]
$e + O_2 \longrightarrow O(^3P) + O(^1D) + e$	$k_{13} = 1.8 \times 10^{-13} \exp(-18.33/T_e)$ m^3 s^{-1}	[11]
$e + O(^3P) \longrightarrow O(^1D) + e$	$k_{14} = 4.5 \times 10^{-15} \exp(-2.29/T_e)$ m^3 s^{-1}	[23]
$O(^1D) + O_2 \longrightarrow O(^3P) + O_2$	$k_{15} = 3.0 \times 10^{-17}$ m^3 s^{-1}	[11]
$O(^1D) + O(^3P) \longrightarrow 2O(^3P)$	$k_{16} = 8.1 \times 10^{-18}$ m^3 s^{-1}	[23]
$e + O(^1D) \longrightarrow O^+ + 2e$	$k_{17} = 9 \times 10^{-15} T_e^{0.7} \exp(-11.6/T_e)$ m^3 s^{-1}	[23]
$e + O_2 \longrightarrow O_2(a^1\Delta_g) + e$	$k_{18} = 1.7 \times 10^{-15} \exp(-3.1/T_e)$ m^3 s^{-1}	[46]
$e + O_2(a^1\Delta_g) \longrightarrow O_2^+ + 2e$	$k_{19} = 9.0 \times 10^{-16} T_e^2 \exp(-11.6/T_e)$ m^3 s^{-1}	[46]
$e + O_2(a^1\Delta_g) \longrightarrow O^- + O$	$k_{20} = 2.28 \times 10^{-16} \exp(-2.29/T_e)$ m^3 s^{-1}	[30]
$e + O_2(a^1\Delta_g) \longrightarrow O_2 + e$	$k_{21} = 5.6 \times 10^{-15} \exp(-2.2/T_e)$ m^3 s^{-1}	[46]
$e + O_2(a^1\Delta_g) \longrightarrow 2O + e$	$k_{22} = 4.2 \times 10^{-15} \exp(-4.6/T_e)$ m^3 s^{-1}	[46]
$O^- + O_2(a^1\Delta_g) \longrightarrow O_2^- + O(^3P)$	$k_{23} = 1.1 \times 10^{-17} (300/T_g)^{1/2}$ m^3 s^{-1}	[41]
$O_2^- + O_2^+ \longrightarrow O_2$	$k_{24} = 2.0 \times 10^{-13} (300/T_g)^{1/2}$ m^3 s^{-1}	[46]
$O_2^- + O^+ \longrightarrow O_2 + O(^3P)$	$k_{25} = 2.0 \times 10^{-13} (300/T_g)^{1/2}$ m^3 s^{-1}	[46]
$e + O_2 + O_2 \longrightarrow O_2^- + O_2$	$k_{26} = 2.26 \times 10^{-42} (300/T_g)^{1/2}$ m^3 s^{-1}	[48]
$O^- + O^+ \longrightarrow O(^3P) + O(^1D)$	$k_{27} = 4.9 \times 10^{-16} (300/T_g)^{1/2}$ m^3 s^{-1}	[43]
$O_2^- + O_2(a^1\Delta_g) \longrightarrow 2O_2 + e$	$k_{28} = 2.7 \times 10^{-17} (300/T_g)^{1/2}$ m^3 s^{-1}	[41]
$O_2^- + O(^3P) \longrightarrow O^- + O_2$	$k_{29} = 3.31 \times 10^{-16} (300/T_g)^{1/2}$ m^3 s^{-1}	[11]
$e + O_3 \longrightarrow O^- + O_2$	$k_{30} = 9.3 \times 10^{-16} / T_e^{0.62}$ m^3 s^{-1}	[45]
$e + O_3 \longrightarrow O + O_2^-$	$k_{31} = 2.0 \times 10^{-16}$ m^3 s^{-1}	[45]
$O^- + O_2 \longrightarrow O_3 + e$	$k_{32} = 5.0 \times 10^{-21} (300/T_g)^{1/2}$ m^3 s^{-1}	[12]
$O^- + O_2(a^1\Delta_g) \longrightarrow O_3 + e$	$k_{33} = 2.2 \times 10^{-17} (300/T_g)^{1/2}$ m^3 s^{-1}	[41]
$O^+ + O_3 \longrightarrow O_2^+ + O_2$	$k_{34} = 1.0 \times 10^{-17} (300/T_g)^{1/2}$ m^3 s^{-1}	[46]
$O + O_3 \longrightarrow 2O_2$	$k_{35} = 2.0 \times 10^{-17} (300/T_g)^{1/2}$ m^3 s^{-1}	[46]
$O^- + O_3 \longrightarrow O_3^- + O$	$k_{36} = 5.3 \times 10^{-16} (300/T_g)^{1/2}$ m^3 s^{-1}	[11]
$O_3^- + O(^3P) \longrightarrow O_2^- + O_2$	$k_{37} = 3.2 \times 10^{-16} (300/T_g)^{1/2}$ m^3 s^{-1}	[12]
$O_3^- + O(^3P) \longrightarrow 2O_2 + e$	$k_{38} = 3.0 \times 10^{-16} (300/T_g)^{1/2}$ m^3 s^{-1}	[12]
$O_3^- + O_2^+ \longrightarrow O_2 + O_3$	$k_{39} = 2 \times 10^{-13} (300/T_g)^{1/2}$ m^3 s^{-1}	[11]
$O_3^- + O_2^+ \longrightarrow 2O + O_3$	$k_{40} = 1.01 \times 10^{-13} (300/T_g)^{1/2}$ m^3 s^{-1}	[11]
$O_2^- + O_3 \longrightarrow O_2 + O_3^-$	$k_{41} = 4 \times 10^{-16} (300/T_g)^{1/2}$ m^3 s^{-1}	[11]
$O_2^- + O(^3P) \longrightarrow O_3 + e$	$k_{42} = 3.01 \times 10^{-16} (300/T_g)^{1/2}$ m^3 s^{-1}	[11]
$e + O_3 \longrightarrow O(^3P) + O_2 + e$	$k_{43} = 1 \times 10^{-14} (300/T_g)^{1/2}$ m^3 s^{-1}	[11]
$2O_2 + O(^3P) \longrightarrow O_3 + O_2$	$k_{44} = 6.9 \times 10^{-40} (300/T_g)^{-1.25} [O_2]$ m^3 s^{-1}	[11]
$O_2^- + 2O(^3P) \longrightarrow O_3 + O(^3P)$	$k_{45} = 3.82 \times 10^{-40} [O]$ m^3 s^{-1}	[11]
$e + O(^3P) + O_2 \longrightarrow O_2^- + O(^3P)$	$k_{46} = 1 \times 10^{-43}$ m^6 s^{-1}	[11]
$e + O(^3P) + O_2 \longrightarrow O^- + O_2$	$k_{47} = 1 \times 10^{-43}$ m^6 s^{-1}	[11]
$e + O_2^+ \longrightarrow O(^1D) + O(^3P)$	$k_{48} = 2.11 \times 10^{-13} (300/T_g)^{0.7}$ m^3 s^{-1}	[11]
$O_2^+ + O(^1D) \longrightarrow O_2(a^1\Delta_g) + O(^3P)$	$k_{49} = 1.0 \times 10^{-18} (300/T_g)^{0.5}$ m^3 s^{-1}	[11]
T_g (K)		
T_e (eV)		

1102

Oxygen discharge

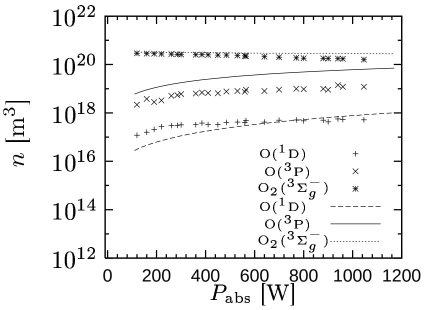

- The neutral densities of atomic and molecular oxygen as well as the lowest excited states versus absorbed power
- The measurements by Fuller et al. [Fuller et al., 2000] was made in an inductively coupled discharge in a cylindrical stainless steel chamber with $R = 18$ cm and $L = 22$ cm. The operating pressure was 10 mTorr

Oxygen discharge

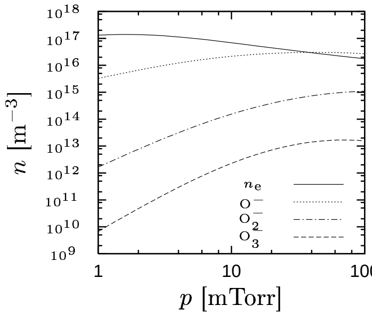

- The densities of electrons n_e and negative oxygen ions, O^-, O_2^-, and O_3^-, versus discharge pressure at 500 W and flowrate 50 sccm for a cylindrical stainless steel chamber with $L = 7.6$ cm and $R = 15.2$ cm

Oxygen discharge

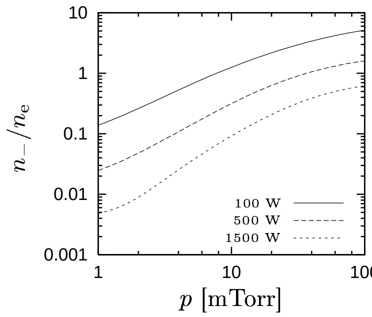

- The electronegativity $n_e/(n_- + n_{2-} + n_{3-})$ at 100, 500 and 1500 W versus discharge pressure
- We assume flowrate to be 50 sccm and a cylindrical stainless steel chamber with $L = 7.6$ cm and $R = 15.2$ cm

Creation - destruction of O^-

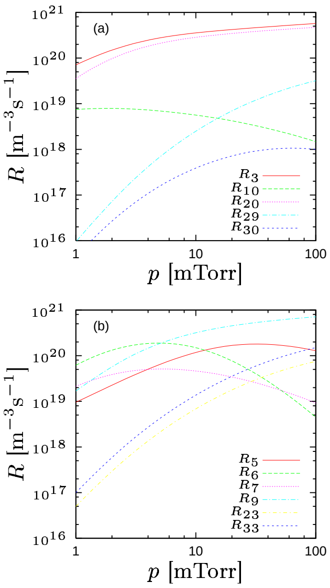

Creation - destruction of O^-

- Creation of the negative ion O^- is mainly through

  $e + O_2(^3\Sigma_g^-) \longrightarrow O(^3P) + O^-$ reaction 3

  og

  $e + O_2(a^1\Delta_g) \longrightarrow O(^3P) + O^-$ reaction 20

  in the pressure range 1 – 100 mTorr

- Destruction is mainly through

  $O^- + O^+ \longrightarrow O(^3P) + O(^3P)$ reaction 6

  at low pressure (< 10 mTorr) and

  $O(^3P) + O^- \longrightarrow e + O_2(^3\Sigma_g^-)$ reaction 9

  og

  $O^- + O_2^+ \longrightarrow O(^3P) + O_2(^3\Sigma_g^-)$ reaction 5

  at higher pressure 10 – 100 mTorr

The metastable $O_2(a^1\Delta_g)$


COMMENT
Is oxygen a detachment-dominated gas or not?

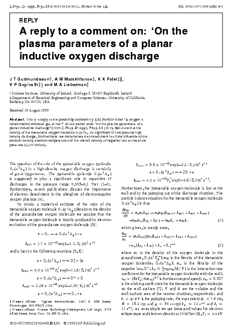
REPLY
A reply to a comment on: 'On the plasma parameters of a planar inductive oxygen discharge'

[Franklin, 2000] and
[Gudmundsson et al., 2000]

The metastable $O_2(a^1\Delta_g)$

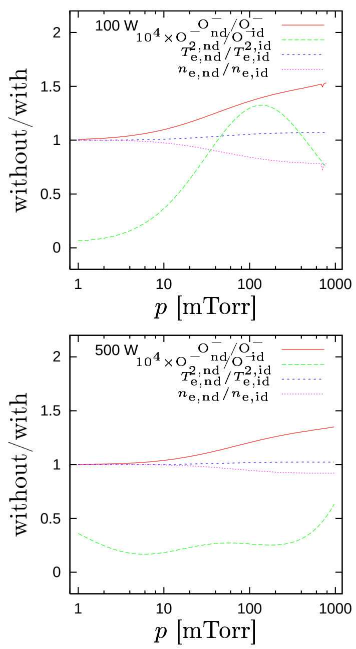

The metastable $O_2(a^1\Delta_g)$

- The model was applied to investigate the influence of the metastable molecule $O_2(a^1\Delta_g)$ on the discharge
- The influence of neglecting the reactions

$$O^- + O_2(a^1\Delta_g) \longrightarrow O_2^- + O \qquad \text{reaction 23}$$

$$O^- + O_2(a^1\Delta_g) \longrightarrow O_3 + e \qquad \text{reaction 33}$$

$$O_2^- + O_2(a^1\Delta_g) \longrightarrow 2O_2 + e \qquad \text{reaction 28}$$

  on the plasma parameters
- The effects are negligible at low pressure but the error increases with increasing pressure

Summary

- The low pressure inductive discharge was introduced
- A first principles electromagnetic model of a planar inductive discharge was described:
  - It was used to calculate the rf voltage and current applied to drive argon discharge
  - It was applied to estimate the current induced in the discharge
- A global model of an oxygen discharge was used to:
  - Investigate creation and destruction of O^-
  - Look at the influence of the metastable molecule $O_2(a^1\Delta_g)$

References

[Amorim et al., 1991] Amorim, J., Maciel, H., and Sudamo, J. (1991). High-density plasma mode of an inductively coupled radio frequency discharge. *Journal of Vacuum Science and Technology B*, 9:362 – 365.

[El-Fayoumi, 1996] El-Fayoumi, I. M. A. (1996). *The electrical and electromagnetic properties of a low frequency, inductively coupled RF plasma source*. PhD thesis, The Flinders University of South Australia.

[Franklin, 2000] Franklin, R. N. (2000). Is oxygen a detachment-dominated gas or not ? *Journal of Physics D: Applied Physics*, 33:3009.

[Fuller et al., 2000] Fuller, N. C. M., Malyshev, M. V., Donnelly, V. M., and Herman, I. P. (2000). Characterization of transformer coupled oxygen plasmas by trace rare gases-optical emission spectroscopy and Langmuir probe analysis. *Plasma Sources Science and Technology*, 9(2):116–127.

[Gudmundsson and Lieberman, 1998] Gudmundsson, J. T. and Lieberman, M. A. (1998). Magnetic induction and plasma impedance in a planar inductive discharge. *Plasma Sources Science and Technology*, 7:83 – 95.

[Gudmundsson et al., 2000] Gudmundsson, J. T., Marakhtanov, A. M., Patel, K. K., Gopinath, V. P., and Lieberman, M. A. (2000). A reply to a comment on: On the plasma parameters of a planar inductive oxygen discharge. *Journal of Physics D: Applied Physics*, 33:3010 – 3012.

[Hittorf, 1884] Hittorf, W. (1884). Ueber die electricitätsleitung der gase. *Annalen der Physik und Chemie*, 21:90 – 139.

[Kortshagen et al., 1996] Kortshagen, U., Gibson, N., and Lawler, J. (1996). On the e-h-mode transition in inductively coupled rf plasmas. *Journal of Physics D: Applied Physics*, 29:1224 – 1236.

[MacKinnon, 1929] MacKinnon, K. (1929). On the origin of the electrodeless discharge. *Philosophical Magazine*, 8:605 – 616.

[Tesla, 1891] Tesla, N. (July 1891). *The Electrical Engineer*, 7:14 – 15.

[Thomson, 1891] Thomson, J. J. (1891). On the discharge of electricity through exhausted tubes without electrodes. *Philosophical Magazine*, 32:321 – 336 and 445 – 464.